AIRS-based versus flask-based estimation of carbon surface fluxes

F. Chevallier, R.J. Engelen, C. Carouge, T. J. Conway, P. Peylin, C. Pickett-Heaps, M. Ramonet, Pj Rayner, Irène Xueref-Remy

AIRS-based versus flask-based estimation of carbon surface fluxes

Frédéric Chevallier,[1] Richard J. Engelen,[2] Claire Carouge,[1] Thomas J. Conway,[3] Philippe Peylin,[1] Christopher Pickett-Heaps,[1] Michel Ramonet,[1] Peter J. Rayner,[1] and Irène Xueref-Remy[1]

Received 24 April 2009; revised 18 July 2009; accepted 27 July 2009; published 23 October 2009.

[1] This paper demonstrates an inversion of surface CO_2 fluxes using concentrations derived from assimilation of satellite radiances. Radiances come from the Atmospheric Infrared Sounder (AIRS) and are assimilated within the system of the European Centre for Medium-Range Weather Forecasts. We evaluate the quality of the inverted fluxes by comparing simulated concentrations with independent airborne measurements. As a benchmark we use an inversion based on surface flask measurements and another using only the global concentration trend. We show that the AIRS-based inversion is able to improve the match to the independent data compared to the prior estimate but that it usually performs worse than either the flask-based or trend-based inversion.

Citation: Chevallier, F., R. J. Engelen, C. Carouge, T. J. Conway, P. Peylin, C. Pickett-Heaps, M. Ramonet, P. J. Rayner, and I. Xueref-Remy (2009), AIRS-based versus flask-based estimation of carbon surface fluxes, *J. Geophys. Res.*, *114*, D20303, doi:10.1029/2009JD012311.

1. Introduction

[2] Chemically, carbon dioxide is an almost stable gas in the atmosphere. The space-time variations of its concentrations are driven by the space-time variations of the fluxes at the Earth surface convolved with atmospheric transport. As a consequence, the CO_2 mole fractions carry integrated information about the carbon fluxes that can be retrieved using statistical inverse methods. Those methods usually implement Bayes' rule by updating some prior knowledge about the fluxes given the available observations and given the error statistics assigned to each piece of information. They were introduced in the 1990s [e.g., *Enting et al.*, 1995] and have been widely used since then [e.g., *Bousquet et al.*, 2000; *Gurney et al.*, 2002; *Denman et al.*, 2007; *Peters et al.*, 2007]. Such studies have motivated an ambitious expansion of the monitoring network at the Earth surface, in the air and from space. The satellite component is emerging with the launch of the first dedicated instrument in January 2009, the Japanese Greenhouse Gases Observing Satellite (GOSAT) [*Yokota et al.*, 2004], and despite the loss of the second one (the U.S. Orbiting Carbon Observatory (OCO)) [*Crisp et al.*, 2004]. In the wake of the preparation for GOSAT and OCO, significant efforts have been put into the exploitation of the existing spaceborne instruments that were designed for other purposes than the observation of carbon but still yield radiances in spectral regions with CO_2 absorption. For instance, CO_2 concentrations in the upper troposphere have been retrieved from the radiation measurements made by the Atmospheric Infrared Sounder (AIRS) [*Engelen et al.*, 2004; *Crevoisier et al.*, 2004; *Chahine et al.*, 2008; *Strow and Hannon*, 2008] and by the Infrared Atmospheric Sounding Interferometer (IASI) [*Crevoisier et al.*, 2009]. At the European Centre for Medium-Range Weather Forecasts (ECMWF) the numerical weather prediction (NWP) system has been extended for the analysis of CO_2 concentrations, based on AIRS and IASI radiance observations [*Engelen et al.*, 2004]. This work paves the way for the exploitation of CO_2 retrievals from GOSAT or from future satellite instruments. However, the direct utility of the current satellite observations to constrain surface carbon flux estimates is still open to question. If useful information on carbon fluxes is available from such instruments, the community could gain several years of additional data at little cost. In two previous studies [*Chevallier et al.*, 2005a, 2005b], we highlighted the large sensitivity of flux inversion systems to regional biases in satellite products. The present paper assesses the usefulness of the AIRS-based analyses of CO_2 concentrations of *Engelen et al.* [2009] over a 3-year period (2003–2005). This product is compared against two other flux fields. The first one is inferred from the NOAA surface network using the same inversion system. The second one is obtained by adjusting the prior field in an empirical manner so that it simply matches the observed atmospheric global growth rate. Aircraft data allow us to discriminate between the three flux fields. Method and data are described in section 2. The results are presented in section 3 and discussed in section 4.

2. Data and Method

2.1. From the AIRS Radiances to the CO_2 Surface Fluxes

2.1.1. AIRS Radiances

[3] The AIRS instrument is part of the NASA Aqua payload. The satellite was launched in May 2002. From the

[1] Laboratoire des Sciences du Climat et de l'Environnement, Gif sur Yvette, France.
[2] European Centre for Medium-Range Weather Forecasts, Reading, UK.
[3] Global Monitoring Division, Earth System Research Laboratory, NOAA, Boulder, Colorado, USA.

0148-0227/09/2009JD012311

2378 channels of the spectrometer, a subset of 324 is received operationally at ECMWF [*McNally et al.*, 2006]. Based on the sensitivity of each channel to the various atmospheric constituents, a selection of 18 channels in the long-wave band and 10 channels in the short-wave band has been made for the CO_2 analysis. Their sensitivity with respect to CO_2 concentrations peaks in the upper troposphere. The other AIRS channels are only used for cloud detection in this setup of the NWP system.

2.1.2. Variational Inference

[4] To infer surface fluxes from the AIRS radiances, a series of two inference systems are used successively: a four-dimensional variational (4D-Var) data assimilation system that analyses the CO_2 atmospheric concentrations and a variational flux inversion system. Even though they involve two different atmospheric models and different space-time scales, both the CO_2 concentration analysis and the CO_2 flux inversion rely on the same Bayesian statistical framework. In both cases a similar cost function J is minimized to find the statistically optimal concentrations and fluxes. J is defined by

$$J(\mathbf{x}) = (\mathbf{x}-\mathbf{x_b})^{\mathrm{T}}\mathbf{B}^{-1}(\mathbf{x}-\mathbf{x_b}) + (H(\mathbf{x})-\mathbf{y})^{\mathrm{T}}\mathbf{R}^{-1}(H(\mathbf{x})-\mathbf{y}), \quad (1)$$

with T the transpose operator, $\mathbf{x}$ the state vector of variables to be optimized, $\mathbf{x_b}$ its prior values, $\mathbf{y}$ the observation vector, H the observation operator that computes the observation equivalent from $\mathbf{x}$, and $\mathbf{B}$ and $\mathbf{R}$ the covariance matrices of the prior and of the observation errors, respectively.

[5] For the analysis of CO_2 concentrations, J is the full 4D-Var cost function of the ECMWF NWP system. The state vector $\mathbf{x}$ includes the 3D CO_2 concentrations at the initial time step of the analysis window and all the standard NWP variables like temperature, humidity and pressure. Note that it does not include the CO_2 surface fluxes which are only optimized in the second inversion system. The observations in $\mathbf{y}$ are not restricted to the AIRS radiances, but gather all standard NWP observations, such as the various microwave sounders, geostationary satellites and radiosonde reports but only the AIRS radiances are directly linked to CO_2 concentration. H is the ECMWF forecast model in combination with the Radiative Transfer for the TIROS Operational Vertical Sounder (RTTOV) [*Matricardi et al.*, 2004, and references therein], upgraded to model the CO_2 transport with prescribed climatological surface fluxes as boundary conditions. The cost function J is minimized for consecutive 12-h time windows. The information, including the CO_2 concentrations, is transferred from one segment to the next via the forecast model. The assimilated AIRS radiances mainly inform about CO_2 in the middle and upper troposphere but thanks to the dynamical analysis of the 12-h 4D-Var and to the prior error correlations, some deeper information is collected lower in the troposphere. The spatial resolution of this study is defined as a reduced Gaussian grid with about 125 km resolution, and 60 vertical levels. The development steps of this system have been reported by *Engelen et al.* [2004], *Engelen and McNally* [2005] and *Engelen et al.* [2009] and will not be further described here.

[6] The 4D-Var approach is usually recognized as the best method to analyze the atmospheric composition. However, exploiting the resulting fields of CO_2 for flux inversion represents an important challenge for two main reasons. First, the error statistics of the analyzed 4D fields are not well known and even if they were, they would represent a wealth of information that would be too large to be processed in the inversion schemes. Second, the CO_2 flux inversion implies modeling the CO_2 transport from the surface to the upper troposphere, where the appropriate AIRS channels are the most sensitive to CO_2. The time scales involved reach weeks or even months, much beyond the 12-h window of the ECMWF 4D-Var. In order to maintain an acceptable computational burden of a single inversion, compromises have to be found that necessarily reduce the optimality of the inversion. Our strategy is described hereafter.

[7] Our CO_2 flux inversion system is based on the work of *Chevallier et al.* [2005b, 2007]. As input, it uses here the CO_2 concentrations analyzed between 200hPa and 500hPa from the 4D-Var at 0000, 0600, 1200 and 1800 UTC and averaged at a $3.75^\circ \times 2.5^\circ$ (longitude-latitude) horizontal resolution. Not all data are fed to the system. First, data south of 20°S are left out because the small variations of the concentrations in these latitudes make the inversion system particularly vulnerable to biases [*Chevallier et al.*, 2005a]. Second, data located beyond 50 degrees north from the equator are also removed because of the small sensitivity of AIRS to CO_2 concentrations there. Note that the inversion system may generate flux increments in data-void areas due to atmospheric transport, but they are likely to be of lesser accuracy than in the directly observed areas. Last, 90% of the remaining column concentrations are randomly removed (thinned) in order to reduce the data volume and to limit the observation error spatial correlations. The thinning is done in such a way that it makes the observation density, in km^{-2}, independent from latitude. As a result, 1,043,529 analyzed values are used for the flux inversion over the three years. The error of the individual data is conservatively set to 3 ppm, i.e., about the variability of the quantity. The error correlations that remain after thinning are neglected. As output, the flux inversion system provides an optimal state vector $\mathbf{x}$ which consists of daytime and nighttime 8-day net total surface fluxes at a $3.75^\circ \times 2.5^\circ$ (longitude-latitude) horizontal resolution throughout the temporal window of the inversion, and of the concentrations at the initial time step of the inversion window. The 8-day resolution is motivated by the large autocorrelations of the prior surface flux errors over days [*Chevallier et al.*, 2006]. The transport is also simplified. $H(\mathbf{x})$ in equation (1) is linearized for the flux inversion around the values of the ECMWF prior concentrations, so that

$$H(\mathbf{x_b}+\delta\mathbf{x}) = H_{ECMWF}(\mathbf{x_b}) + \mathbf{H}_{\mathrm{LMDZ}}(\mathbf{x_b})\delta\mathbf{x}. \quad (2)$$

In equation (2), $\delta\mathbf{x}$ represents any flux increment in the inversion system. H_{ECMWF} is the ECMWF transport model. $\mathbf{H}_{\mathrm{LMDZ}}(\mathbf{x_b})$ is the Jacobian matrix of the transport model of the Laboratoire de Météorologie Dynamique (LMDZ) [*Hourdin et al.*, 2006] nudged to ECMWF winds and with the boundary conditions defined from $\mathbf{x_b}$. The standard version of LMDZ currently uses 19 vertical levels and a horizontal resolution of 3.75° in longitude and 2.5° in latitude. It has been validated against aircraft [*Peylin et al.*, 2007; *Stephens et al.*, 2007] and, together with the ECMWF transport model, against surface measurements [*Law et al.*, 2008; *Patra et al.*, 2008]. The model is here ran in an off-line mode (transport mass fluxes

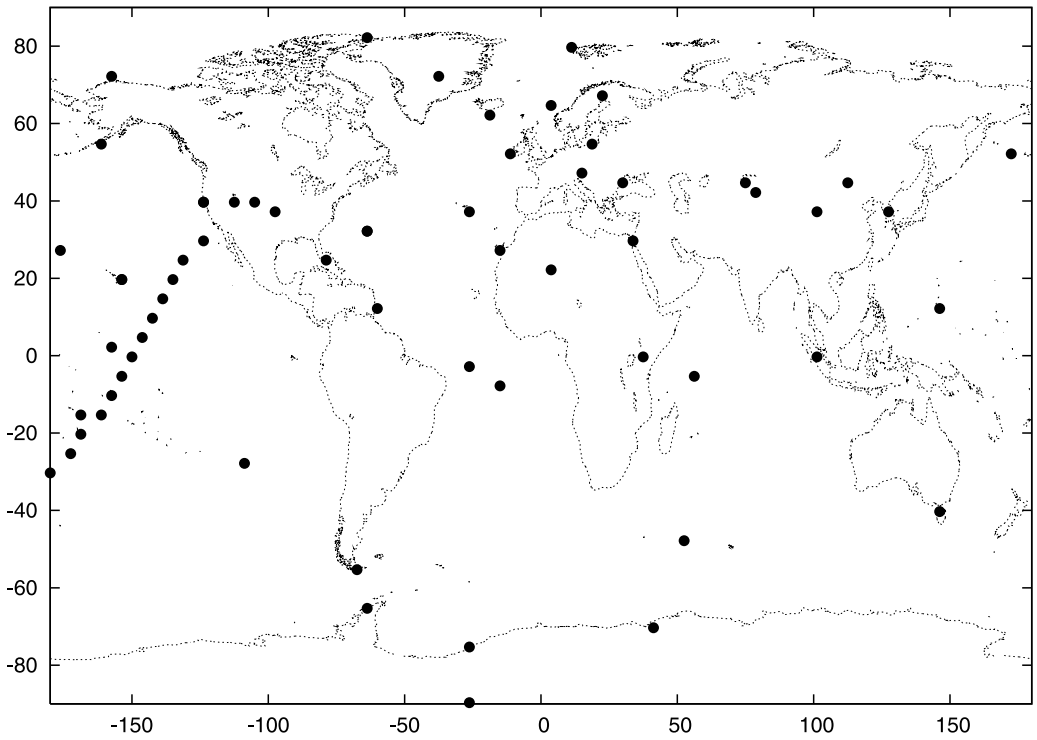

Figure 1. Location of the NOAA ESRL flask measurements used in this study.

are read from a frozen archive rather than computed online). This linearization strategy is inspired by the ECMWF incremental 4D-Var where the prior state of the model is computed at the highest affordable resolution with the full forecast model and increments are computed at lower resolution with a simplified model [*Courtier et al.*, 1994].

[8] Despite their differences, effort has been made to homogenize the concentration analysis system and the flux inversion system. This is all the more important since the information content of AIRS about surface fluxes is small [*Chevallier et al.*, 2005a] and artificial patterns can easily be introduced in the analyzed fluxes. The linearization strategy of equation (2) illustrates this effort. Further, the same prior surface fluxes (anthropogenic from http://cdiac.esd.ornl.gov/ndps/ndp058a.html, air-sea exchange from http://www.ldeo.columbia.edu/res/pi/CO2/carbondioxide/air_sea_flux/fluxdata.txt, terrestrial ecosystem exchange from the Carnegie Ames Stanford Approach model (CASA) [*Randerson et al.*, 1997] and biomass burning from http://www.daac.ornl.gov/VEGETATION/guides/global_fire_emissions_v2.1.html) are used in both systems as boundary condition for the transport simulation. Finally, the concentrations at the initial time step of the flux inversion window come from the ECMWF system. It is noteworthy that the CASA fluxes used here are annually balanced over land and do not simulate the recovery of burned vegetation. Therefore, they miss a global land sink of about 3 GtC per year that the inversion system has to infer from the atmospheric observations.

2.1.3. Statistics of the Prior Flux Errors

[9] The error statistics of the above-described prior fluxes are a key component of the inversion system and they have been carefully modeled by a multivariate Gaussian distribution. Over land, its parameters are inspired by the comparison between in situ flux measurements and the outputs of a biosphere model that was reported by *Chevallier et al.* [2006]: temporal correlations decay exponentially with a length of one month but nighttime errors are assumed to be uncorrelated with daytime errors; spatial correlations decay exponentially with a length of 500 km (i.e., about the east-west size of the transport model grid at the equator); and standard deviations are set proportional to the heterotrophic respiration (the scaling factor, deduced from the data of *Chevallier et al.* [2006], is 2.5), with maximum authorized error values of 9 $gC.m^{-2}$ per day. Over a full year, the total uncertainty for all land fluxes amounts to about 4.5 GtC. Ocean error statistics are more arbitrary and the following parameters have been chosen: temporal correlations decay exponentially with a length of 1 month; unlike land, daytime and nighttime flux errors are correlated; spatial correlations follow an e-folding length of 1000 km; and standard deviations are set to 0.2 $gC.m^{-2}$ per day. With this setup, the ocean uncertainty amounts to about 1.0 GtC per year. Land and ocean fluxes are not correlated. Note that the prior fluxes are used both in the 4D-Var and in the flux inversion. Therefore there exists some correlations between $\mathbf{y}$ and $\mathbf{x_b}$ for the flux inversion. They are neglected, thereby assuming that the assimilation of AIRS actually drives the 4D-Var error budget.

2.2. From the Surface Measurements to the CO_2 Surface Fluxes

2.2.1. Surface Flask Measurements

[10] The surface measurements are mixing ratios (expressed as dry mole fractions) in individual samples of air collected about every week in various places in the world over land (from four baseline observatories and tens of cooperative fixed sites) and over ocean (from commercial ships), as part of the NOAA/ESRL cooperative air sampling network. Data for the 63 locations shown in Figure 1 have been

Table 1. Characteristics of the Eight Aircraft Campaigns Selected From the GEOMON CO_2 Airborne Data Archive[a]

Mission/Reference	Locality	Organization	Principal Investigator
	Regular Campaigns		
GRI	Scotland, UK	CarboEurope	P. Ciais
HNG	Hungary	CarboEurope	P. Ciais
ORL	Orléans, France	CarboEurope	P. Ciais
	Intensive Campaigns		
CERES	Western Europe May–June 2005	BGC-MPI	C. Gerbig
INTEX-NA, *Singh et al.* [2006]	North America July–August 2004	NASA	S. Vay
PRE-AVE, *Park et al.* [2007]	North America January 2004	Harvard Univ.	S. Wofsy
COBRA-2003, *Matross et al.* [2006], *Miller et al.* [2008], http://www.fas.harvard.edu/~cobra/	North America May–June 2003	Harvard Univ.	S. Wofsy
COBRA-2004	North America May–August 2004	Harvard Univ.	S. Wofsy

[a]An intensive campaign type is a campaign for which the airborne measurements have been obtained during a single intensive period. In this case, the sampling is made of horizontal transects and vertical profiles generally flown over a large area. In a "regular" campaign type, airborne measurements are obtained systematically as part of a regular program (e.g., vertical profiles flown weekly over a single location).

downloaded from ftp://ftp.cmdl.noaa.gov/ccg/co2/flask/ for the studied period (2003–2005). The stations left out had very few or no data for the period of study. The measurements have been screened automatically for the inversion by comparison with the mole fractions calculated by LMDZ from the prior fluxes: a minority of them (about 100 data) was rejected, likely because the transport model was not able to reproduce some local signals. A total of 8155 individual measurements are kept. They are used in the inversion system as they are provided by NOAA/ESRL, without any correction or smoothing. The uncertainty assigned to each observation within the inversion system includes the error of the measurement, the error of the transport model that simulates it and the representativeness error (i.e., the mismatch between the scale of the measurement and the scale of the transport model). It is assumed here to have the same statistical characteristics as the high-frequency variability of the deseasonalized and detrended time series of the measurement at a given station. The high-frequency variability is calculated following *Masarie and Tans* [1995]. The resulting error varies between a few tenths of a ppm for marine stations (e.g., 0.67 ppm at MLO station, in Hawaii) and several ppm for continental ones, reaching 11 ppm at BSC station, in Romania). Error correlations are neglected.

2.2.2. Inference System

[11] To infer the surface fluxes from the surface measurements, the flux inversion system is used directly without the linearization around the ECMWF concentrations of equation (2). The prior fluxes and their statistics are those described above. The reasons for the sole use of the LMDZ model without the ECMWF 4D-Var for this part of the study are twofold. First, there is no need to analyze other variables than CO_2 when dealing with surface measurements, as is the case when AIRS radiances are exploited. Second, the assimilation of surface concentrations in the 4D-Var is not a straightforward task and remains a topic for future research, in contrast to the LMDZ model for which a long experience has been gained.

2.3. Poor Man's Method

[12] In order to establish some baseline standard for the inverted flux fields, a poor man's inversion system is also built in the following way. The ocean fluxes are kept identical to the prior ones. Over land, the inverted fluxes $\mathbf{x_{pm}}$ are defined as

$$\mathbf{x_{pm}} = \mathbf{x_b} - k\boldsymbol{\sigma}, \tag{3}$$

where k is a unique scaling factor and $\boldsymbol{\sigma}$ is the vector made of the prior error standard deviations, i.e., the square root of the diagonal of $\mathbf{B}$. Here k was chosen by trial and error so that the mean global total of the $\mathbf{x_{pm}}$ fluxes equals the mean global total of fluxes inverted from the surface measurements over the 3-year period. A value of 1/55 was found. This simple approach aims at matching the mean global growth rate of CO_2, which is too large with our prior fluxes over land (see the end of section 2.1.2), without any spatial or temporal information from the observations. In practice, it distributes the land carbon sink according to the gross carbon fluxes from the vegetation.

2.4. Aircraft Data

[13] In this study, independent aircraft data are primarily used to evaluate flux estimates and in particular, to gauge the improvement against the prior estimates. The aircraft data used were all obtained from the CO_2 Airborne Data Archive for the period of 2003–2004. This database, containing publicly available CO_2 and CH_4 airborne data from over 50 separate measurement campaigns, was created as part of the pan-European project GEOMON (http://geomon-wg.ipsl.jussieu.fr/). Information related to the specific aircraft data used here is listed in Table 1.

3. Results

[14] Figure 2 displays the mean flux increments from the three data sources. The AIRS-based inversion (top map) has the largest horizontal gradients with peak-to-peak amplitude about 1000 gC m^{-2} per year. The map has a rather zonal pattern of positive values in the tropics and negative ones elsewhere, modulated by the vegetation pattern of the prior error variances. Figure 2 (middle) for the in situ–based inversion shows peak-to-peak amplitude of about 300 gC m^{-2} per year, with mostly negative values that follow the pattern of the prior error variances. Positive values are found in tropical America and, to a smaller extent, in Europe, North

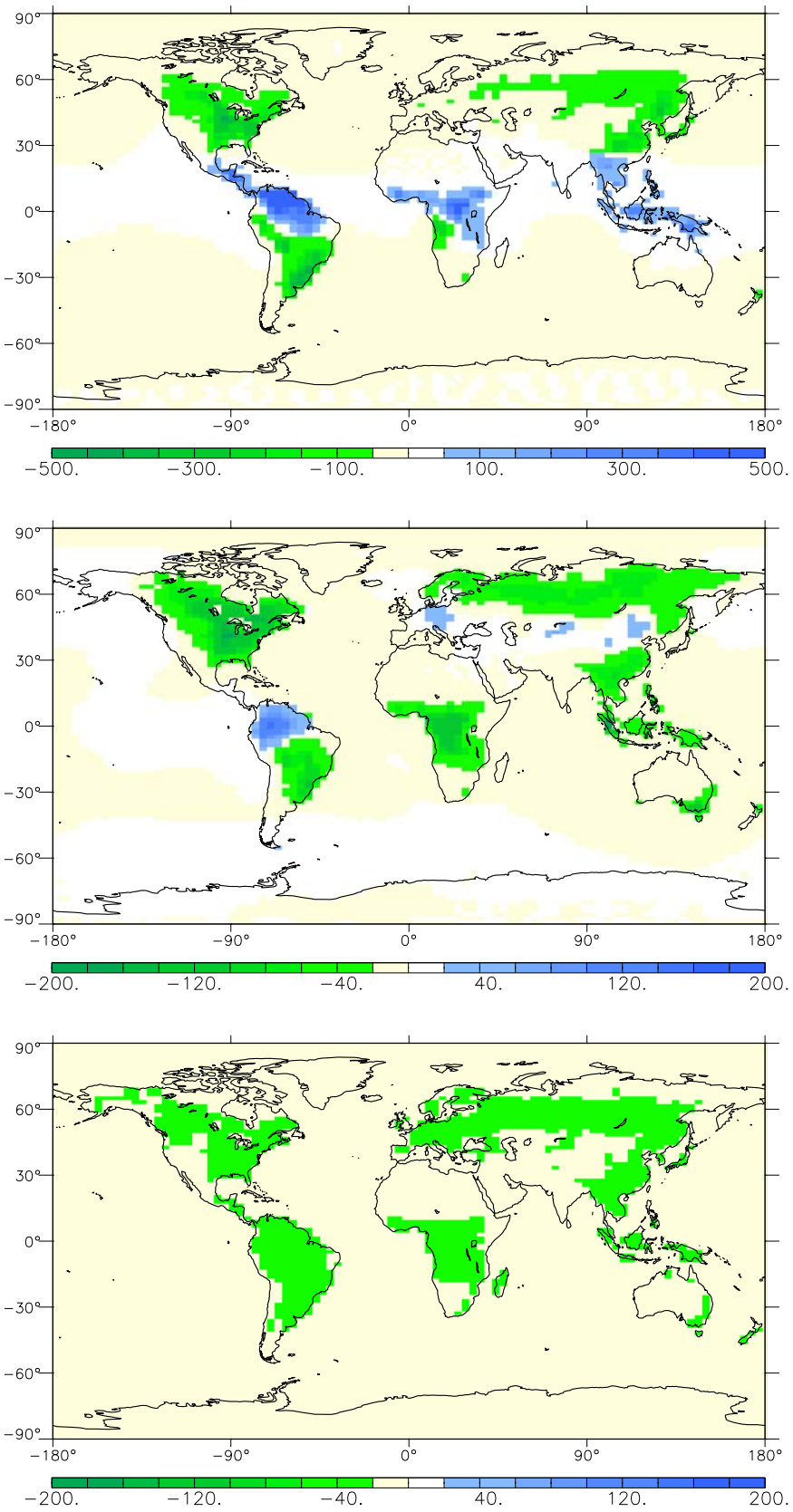

Figure 2. Mean flux increment, in gC m^{-2} per year, (top) from the AIRS data, (middle) from the surface data, and (bottom) from the poor man's method. Note that the range of values for the top map is 2.5 times as large as for the two other maps. Positive (blue) values represent increased sources or decreased sinks.

Table 2. Mean Carbon Budget of the Prior Fluxes and of the Three Flux Inversions[a]

	Prior	AIRS	Surface	Poor Man's Method
Global	7.78	7.17	4.54	4.62
Ocean	−1.54	−1.88	−1.61	−1.54
NH land	6.41	2.93	4.52	4.98
Tropical land	2.58	6.59	1.57	1.12
SH land	0.33	−0.47	0.06	0.06

[a]Over the globe, over the oceans, and in three regions: the land north of 20°N (NH land), the land within 20° of the equator (tropical land), and the land south of 20°S (SH land). Unit is GtC per year.

America or Asia. By construction (see section 2.1.3), the map of the poor man's method (Figure 2, bottom) displays a vegetation pattern with negative values between zero and 70 gC m^{-2} per year.

[15] The budget of the prior fluxes and of the three inversions is summarized in Table 2. As explained in section 2.1.2, the prior fluxes miss several types of sinks and integrate to a large number (7.78 GtC per year). The AIRS total (7.17 GtC per year) is smaller by 8% only, in contrast to the two other inversions that diminish the mean CO_2 flux by about 40%. The AIRS inversion significantly modifies the latitudinal gradient over land by moving the maximum from the Northern latitudes to the tropics, whereas the other two only dampen the prior gradient. Note that the flask inversion provides figures in line with the recent inversion results based on flask and in situ measurements shown on the Carboscope tool (http://www.carboscope.eu/).

[16] High-quality flux measurements are only available at small scales on the order of 1 km^2. Given the flux spatial heterogeneity, they cannot be used to validate the inversions made at a resolution of 3.75° × 2.5°. The aircraft and flask mole fraction measurements allow us to indirectly evaluate the quality of the analyzed fluxes. In this case we use the LMDZ transport model with prior and inverted fluxes successively as boundary conditions.

[17] Figure 3 shows the posterior biases and standard deviations of the differences as a function of the corresponding prior error statistics at each NOAA surface station for the 2003–2005 period. As expected, the flask-based inversion, using these surface data, shows the best improvement from the prior to the posterior with RMS reductions of about 2 ppm. The 2-ppm RMS improvement can be put in perspective with the 6-ppm trend of CO_2 during the 3 years, observed at the surface stations. The AIRS-based inversion did not use these data and shows an improvement at most stations up to about 1 ppm only (consistent with its high surface budget seen in Table 2). Degraded statistics (by a few tenths of a ppm) are seen at six stations among the 63: in the central Pacific (at Christmas Island and for two cruise data) in Romania, in Hungary, and in the United States (Key Biscayne, Florida, and Point Arena, California). The poor man's method, that used some limited information from the flask data, shows intermediate skill between the surface inversion and the AIRS one. For the three inversions, the RMS improvement is obtained from a reduction of both the bias and the standard deviation.

[18] Finally, the three posterior simulations and the prior simulation are compared to the aircraft data (Figures 4 and 5). The eight campaigns rank the flux sets in the same order as the surface data. The posterior fluxes systematically improve on the prior, except at levels very close to the surface and at 700 hPa for ORL. The in situ–based inversion shows the largest improvement for all campaigns but PRE-AVE and COBRA-2003, where it may suffer from the sparseness of the surface network or from deficiencies in the transport model. This inversion usually improves the root mean square error (RMS) by about 1 to 3 ppm, which is consistent with the previous statistics given by the surface data. The AIRS-based inversion improves the RMS compared to the prior by 0.5 to 2 ppm at most levels. The AIRS curves illustrate the successful propagation of the 200–500hPa 4D-Var information down to the lower troposphere. This is achieved by a much longer temporal window in the flux inversion than in the

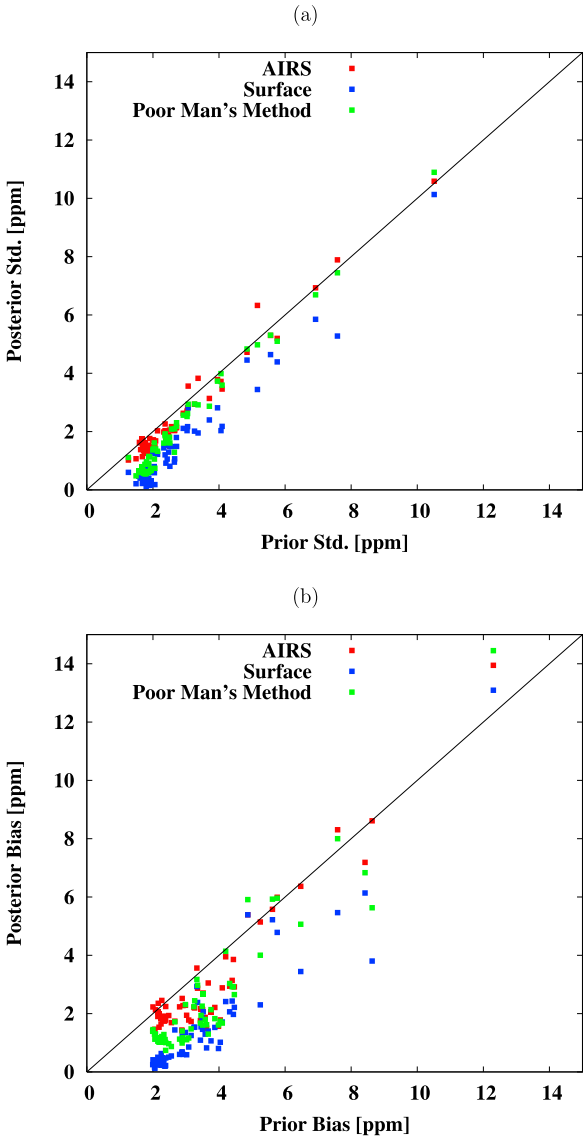

Figure 3. Statistics of the differences between LMDZ simulations and individual surface flask measurements. The LMDZ simulations use the prior fluxes (abscissa) or one of the posterior flux sets as boundary conditions (ordinate). The transport model is run at horizontal resolution 3.75° × 2.5° with 19 levels in the vertical. One point shows (a) the standard deviation or (b) the bias for the 2003–2005 period at one of the 63 NOAA stations.

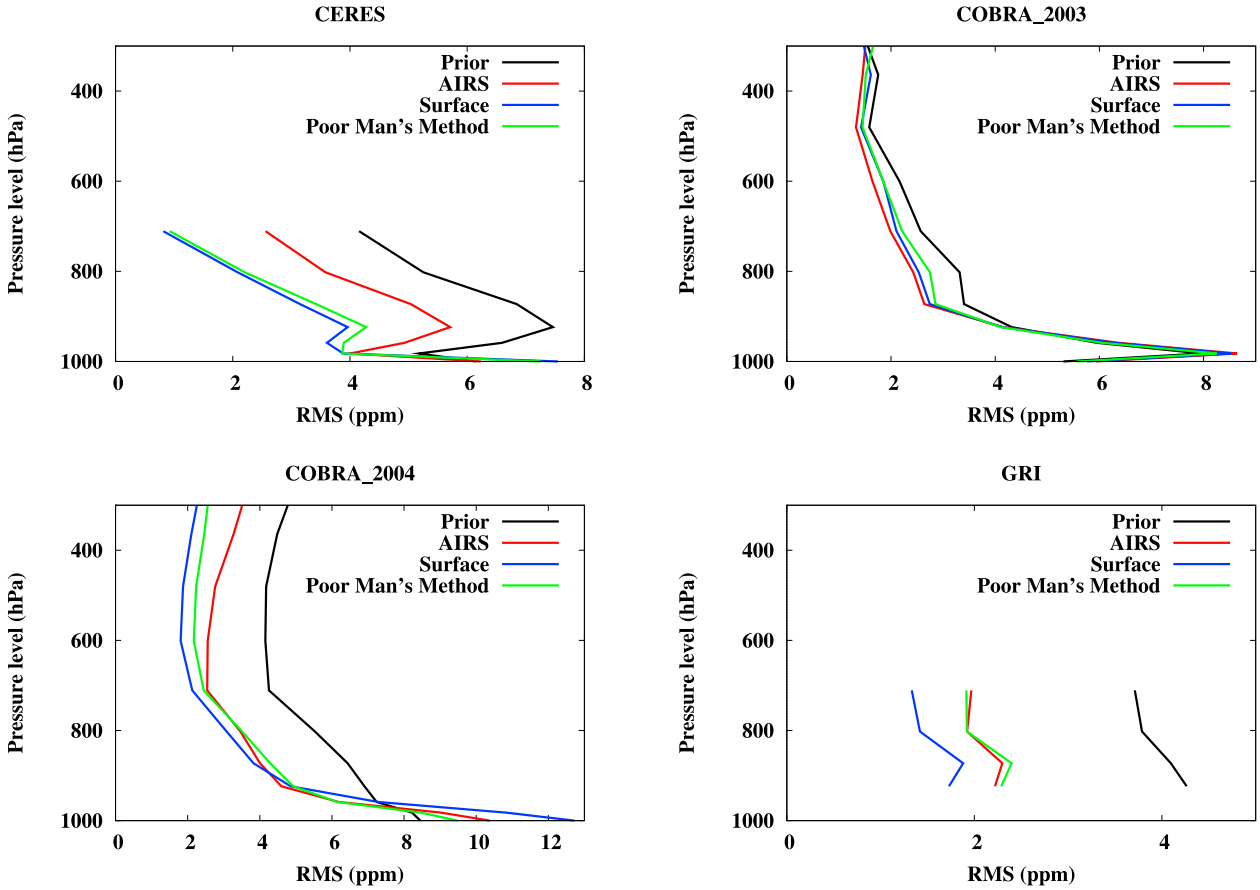

Figure 4. RMS difference between LMDZ simulations and four aircraft measurement campaigns between 2003 and 2005. The LMDZ simulations use the prior fluxes or one of the posterior flux sets as boundary conditions. The transport model is run at horizontal resolution 3.75° × 2.5° with 19 levels in the vertical.

4D-Var (3 years versus 12 h). It outperforms the in situ–based inversion for PRE-AVE below 700hPa and (to a smaller extent) for COBRA-2003 in the free troposphere. In contrast to the results of Figure 3, the AIRS inversion shows rather similar quality on average as the poor man's method. As in section 2, the RMS improvement for the three inversions stems from a reduction of both the bias and the standard deviation (not shown).

4. Conclusion

[19] Among other influences, CO_2 concentrations in the atmosphere affect the radiance measurements of several past or existing space sounders. Extracting such information to monitor CO_2 fluxes at the Earth surface has been a challenge for several years. *Chevallier et al.* [2005b] exploited data from the TIROS Operational Vertical Sounder (TOVS) to tentatively infer the CO_2 fluxes. Together with the study by *Engelen et al.* [2009], this paper focuses on the AIRS space-borne instrument for this same purpose. A two-step approach is proposed that relies on the ECMWF 12-h 4D-Var to extract the information about CO_2 concentration in an optimal way and on a several-year-long variational inversion scheme to extend the analysis to the surface fluxes. Efforts have been made to homogenize the two steps, but the transition is not seamless, in particular for the error statistics of the CO_2 concentration fields and for the transport model. The compromises found so far will further evolve in the future, and the current study marks where we stand now.

[20] The AIRS-based inversion is evaluated by a comparison with two other inversions. The two reference inversions use surface flask measurements with or without any space-time resolution. Consistent with its much higher spectral resolution [*Engelen and Stephens*, 2004], the AIRS instrument shows much better capability to inform about the surface fluxes than TOVS. Compared to the flask inversions, the AIRS inversion provides larger corrections of both signs to our prior surface fluxes. The carbon budget of the AIRS inversion appears to be less realistic than the one from the flask inversion. However, comparisons with independent measurements indicate that the changes do improve the quality of atmospheric simulations, though with a smaller extent than the flask network. The inversion that simply adjusts the atmospheric growth rate without any space-time resolution from observations shows intermediate skill between the two other inversions, or even less than AIRS, depending on the validation data. The AIRS retrievals, measuring the global growth rate with less accuracy, even in the high troposphere, do not allow the inversion system to achieve the same performance than the surface network. When looking at higher-resolution signals, the main difference between the flask-based and the AIRS-based flux inversion lies

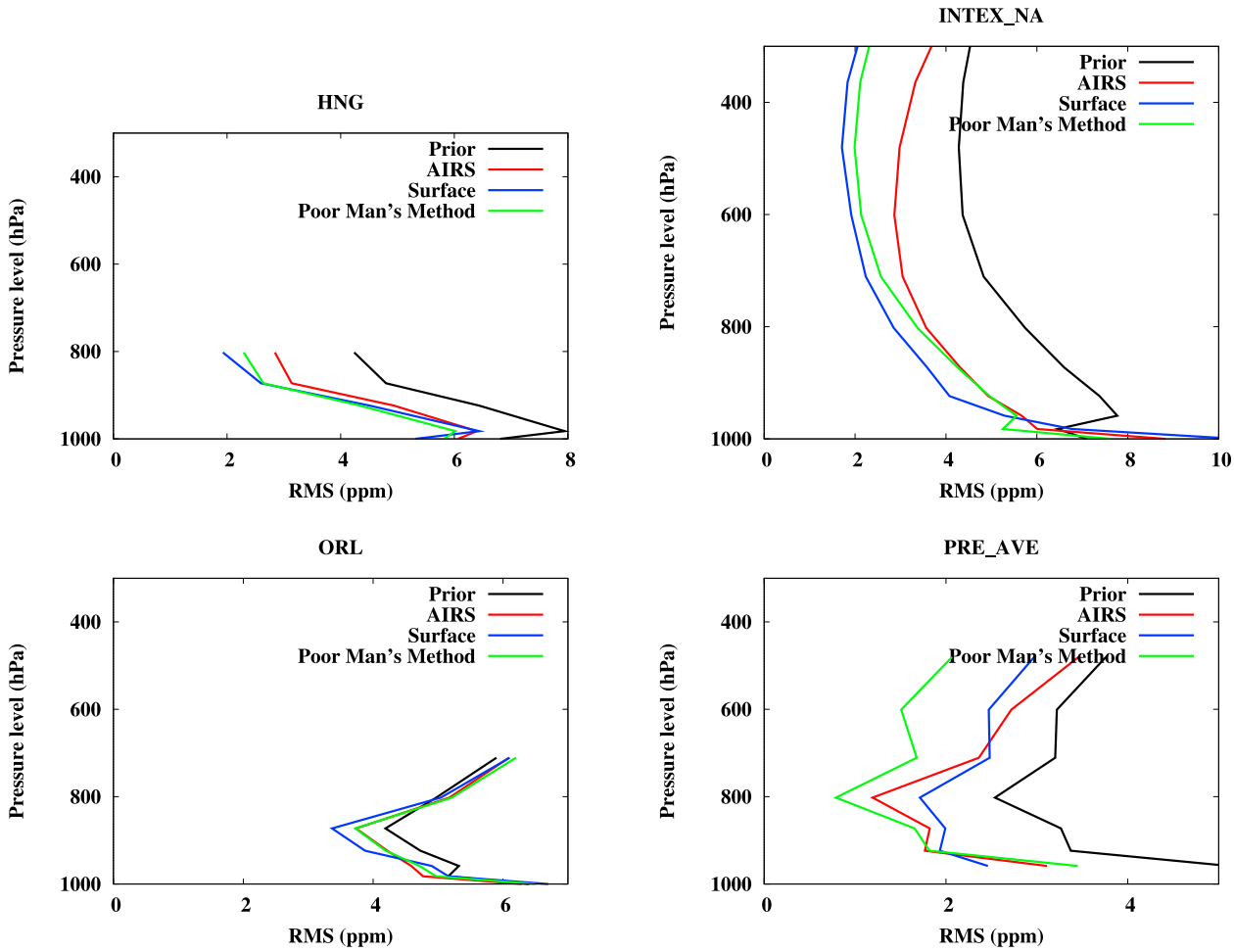

Figure 5. Same as Figure 4 but for four other campaigns.

in the tropics where the two inversions provide mean increments of opposite signs. This part of the globe is poorly observed by conventional measurements, particularly in Africa and Asia. Validation data would be highly beneficial to discriminate between the products in these sparsely observed regions. This recommendation is supported by increased performance of the AIRS product with respect to the PRE-AVE campaign in Central America, a region also poorly observed by conventional methods.

[21] The exploitation of the AIRS radiances does not seem mature enough yet to increase the wealth of knowledge about the global carbon cycle. However, all the components of the system will further evolve in the future. In the mean time, the exploitation of more CO_2-informative data, like the forthcoming GOSAT retrievals in synergy with surface observations, is the next step.

[22] **Acknowledgments.** This study has been cofunded by the European Commission under the GEMS project (contract SIP4-CT-2004-516099). As with previous studies, this study clearly demonstrates the benefits that come from the public availability of, in this case, airborne data. The authors are grateful to the principal investigators of the aircraft campaigns who have made their data publicly available for this study. These people include Philippe Ciais (LSCE) and others involved in the CarboEurope project (GRI, HNG, ORL), Christoph Gerbig (MPI-GBC), Stephanie Vay (NASA LaRC), and Steve Wofsy (Harvard University). The authors would also like to thank F. Marabelle (LSCE) for computer support. Stephanie Vay and three anonymous reviewers helped to improve the clarity of the manuscript.

References

Bousquet, P., P. Peylin, P. Ciais, C. Quere, P. Friedlingstein, and P. Tans (2000), Regional changes in carbon dioxide fluxes of land and oceans since 1980, *Science*, *290*, 1342–1346, doi:10.1126/science.290.5495.1342.

Chahine, M. T., L. Chen, P. Dimotakis, X. Jiang, Q. Li, E. T. Olsen, T. Pagano, J. Randerson, and Y. L. Yung (2008), Satellite remote sounding of mid-tropospheric CO_2, *Geophys. Res. Lett.*, *35*, L17807, doi:10.1029/2008GL035022.

Chevallier, F., R. J. Engelen, and P. Peylin (2005a), The contribution of AIRS data to the estimation of CO_2 sources and sinks, *Geophys. Res. Lett.*, *32*, L23801, doi:10.1029/2005GL024229.

Chevallier, F., M. Fisher, P. Peylin, S. Serrar, P. Bousquet, F.-M. Bréon, A. Chédin, and P. Ciais (2005b), Inferring CO_2 sources and sinks from satellite observations: Method and application to TOVS data, *J. Geophys. Res.*, *110*, D24309, doi:10.1029/2005JD006390.

Chevallier, F., N. Viovy, M. Reichstein, and P. Ciais (2006), On the assignment of prior errors in Bayesian inversions of CO_2 surface fluxes, *Geophys. Res. Lett.*, *33*, L13802, doi:10.1029/2006GL026496.

Chevallier, F., F.-M. Bréon, and P. J. Rayner (2007), Contribution of the Orbiting Carbon Observatory to the estimation of CO_2 sources and sinks: Theoretical study in a variational data assimilation framework, *J. Geophys. Res.*, *112*, D09307, doi:10.1029/2006JD007375.

Courtier, P., J.-N. Thépaut, and A. Hollingworth (1994), A strategy for operational implementation of 4D-Var using an incremental approach, *Q. J. R. Meteorol. Soc.*, *120*, 1367–1387, doi:10.1002/qj.49712051912.

Crevoisier, C., S. Heilliette, A. Chédin, S. Serrar, R. Armante, and N. A. Scott (2004), Midtropospheric CO_2 concentration retrieval from AIRS observations in the tropics, *Geophys. Res. Lett.*, *31*, L17106, doi:10.1029/2004GL020141.

Crevoisier, C., A. Chédin, H. Matsueda, T. Machida, R. Armante, and N. A. Scott (2009), First year of upper tropospheric integrated content of CO_2 from IASI hyperspectral infrared observations, *Atmos. Chem. Phys. Discuss.*, *9*, 8187–8222.

Crisp, D., et al. (2004), The Orbiting Carbon Observatory (OCO) mission, *Adv. Space Res.*, *34*, 700–709, doi:10.1016/j.asr.2003.08.062.

Denman, K. L., et al. (2007), Couplings between changes in the climate system and biogeochemistry, in *Climate Change 2007: The Physical Science Basis. Contribution of Working Group I to the Fourth Assessment Report of the Intergovernmental Panel on Climate Change*, edited by S. Solomon et al., pp. 499–587, Cambridge Univ. Press, Cambridge, U. K.

Engelen, R. J., and A. P. McNally (2005), Estimating atmospheric CO_2 from advanced infrared satellite radiances within an operational four-dimensional variational (4D-Var) data assimilation system: Results and validation, *J. Geophys. Res.*, *110*, D18305, doi:10.1029/2005JD005982.

Engelen, R. J., and G. L. Stephens (2004), Information content of infrared satellite sounding measurements with respect to CO_2, *J. Appl. Meteorol.*, *43*, 373–378, doi:10.1175/1520-0450(2004)043<0373:ICOISS>2.0.CO;2.

Engelen, R. J., E. Andersson, F. Chevallier, A. Hollingsworth, M. Matricardi, A. P. McNally, J.-N. Thépaut, and P. D. Watts (2004), Estimating atmospheric CO_2 from advanced infrared satellite radiances within an operational 4D-Var data assimilation system: Methodology and first results, *J. Geophys. Res.*, *109*, D19309, doi:10.1029/2004JD004777.

Engelen, R. J., S. Serrar, and F. Chevallier (2009), Four-dimensional data assimilation of atmospheric CO_2 using AIRS observations, *J. Geophys. Res.*, *114*, D03303, doi:10.1029/2008JD010739.

Enting, I. G., C. M. Trudinger, and R. J. Francey (1995), A synthesis inversion of the concentration and $\delta^{13}C$ atmospheric CO_2, *Tellus, Ser. B*, *47*, 35–52.

Gurney, K. R., et al. (2002), Towards robust regional estimates of CO_2 sources and sinks using atmospheric transport models, *Nature*, *415*(6872), 626–630, doi:10.1038/415626a.

Hourdin, F., et al. (2006), The LMDZ4 general circulation model: Climate performance and sensitivity to parametrized physics with emphasis on tropical convection, *Clim. Dyn.*, *27*, 787–813, doi:10.1007/s00382-006-0158-0.

Law, R. M., et al. (2008), TransCom model simulations of hourly atmospheric CO_2: Experimental overview and diurnal cycle results for 2002, *Global Biogeochem. Cycles*, *22*, GB3009, doi:10.1029/2007GB003050.

Masarie, K. A., and P. P. Tans (1995), Extension and integration of atmospheric carbon dioxide data into a globally consistent measurement record, *J. Geophys. Res.*, *100*(D6), 11,593–11,610, doi:10.1029/95JD00859.

Matricardi, M., F. Chevallier, G. Kelly, and J.-N. Thépaut (2004), An improved general fast radiative transfer model for the assimilation of radiance observations, *Q. J. R. Meteorol. Soc.*, *130*, 153–173, doi:10.1256/qj.02.181.

Matross, D. M., et al. (2006), Estimating regional carbon exchange in New England and Quebec by combining atmospheric, ground-based, and satellite data, *Tellus, Ser. B*, *58*, 344–358.

McNally, A. P., et al. (2006), The assimilation of AIRS radiance data at ECMWF, *Q. J. R. Meteorol. Soc.*, *132*, 935–957, doi:10.1256/qj.04.171.

Miller, S. M., et al. (2008), Sources of carbon monoxide and formaldehyde in North America determined from high-resolution atmospheric data, *Atmos. Chem. Phys. Discuss.*, *8*, 11,395–11,451.

Park, S., et al. (2007), The CO_2 tracer clock for the Tropical Tropopause Layer, *Atmos. Chem. Phys.*, *7*, 3989–4000.

Patra, P. K., et al. (2008), TransCom model simulations of hourly atmospheric CO_2: Analysis of synoptic-scale variations for the period 2002–2003, *Global Biogeochem. Cycles*, *22*, GB4013, doi:10.1029/2007GB003081.

Peters, W., et al. (2007), An atmospheric perspective on North American carbon dioxide exchange: CarbonTracker, *Proc. Natl. Acad. Sci. U. S. A.*, *104*, 18,925–18,930, doi:10.1073/pnas.0708986104.

Peylin, P., F. M. Bréon, S. Serrar, Y. Tiwari, A. Chédin, M. Gloor, T. Machida, C. Brenninkmeijer, A. Zahn, and P. Ciais (2007), Evaluation of Television Infrared Observation Satellite (TIROS-N) Operational Vertical Sounder (TOVS) spaceborne CO_2 estimates using model simulations and aircraft data, *J. Geophys. Res.*, *112*, D09313, doi:10.1029/2005JD007018.

Randerson, J. T., M. V. Thompson, T. J. Conway, I. Y. Fung, and C. B. Field (1997), The contribution of terrestrial sources and sinks to trends in the seasonal cycle of atmospheric carbon dioxide, *Global Biogeochem. Cycles*, *11*(4), 535–560, doi:10.1029/97GB02268.

Singh, H. B., W. H. Brune, J. H. Crawford, D. J. Jacob, and P. B. Russell (2006), Overview of the summer 2004 Intercontinental Chemical Transport Experiment–North America (INTEX-A), *J. Geophys. Res.*, *111*, D24S01, doi:10.1029/2006JD007905.

Stephens, B. B., et al. (2007), Weak northern and strong tropical land carbon uptake from vertical profiles of atmospheric CO_2, *Science*, *316*, 1732–1735, doi:10.1126/science.1137004.

Strow, L. L., and S. E. Hannon (2008), A 4-year zonal climatology of lower tropospheric CO_2 derived from ocean-only Atmospheric Infrared Sounder observations, *J. Geophys. Res.*, *113*, D18302, doi:10.1029/2007JD009713.

Yokota, T., H. Oguma, I. Morino, and G. Inoue (2004), A nadir looking SWIR FTS to monitor CO_2 column density for Japanese GOSAT project, paper presented at Twenty-Fourth International Symposium on Space Technology and Science, Jpn. Soc. for Aeronaut, and Space Sci., Tokyo.

C. Carouge, F. Chevallier, P. Peylin, C. Pickett-Heaps, M. Ramonet, P. J. Rayner, and I. Xueref-Remy, Laboratoire des Sciences du Climat et de l'Environnement, bat 701, L'Orme des Merisiers, F-91191 Gif Sur Yvette, France. (frederic.chevallier@lsce.ipsl.fr)

T. J. Conway, Global Monitoring Division, Earth System Research Laboratory, NOAA, 325 Broadway, Boulder, CO 80305, USA.

R. J. Engelen, European Centre for Medium-Range Weather Forecasts, Shinfield Park, Reading RG2 9AX, UK.